

## Effect of a proximal substrate on plasmon propagation in silver nanowires

Zhipeng Li,<sup>1</sup> Kui Bao,<sup>2,3</sup> Yurui Fang,<sup>1</sup> Zhiqiang Guan,<sup>1</sup> Naomi J. Halas,<sup>2,3,1,\*</sup> Peter Nordlander,<sup>2,3,1,\*</sup>† and Hongxing Xu<sup>1,4,\*</sup>‡

<sup>1</sup>Beijing National Laboratory for Condensed Matter Physics, Institute of Physics, Chinese Academy of Sciences, P.O. Box 603-146, 100190 Beijing, China

<sup>2</sup>Department of Physics and Astronomy, Laboratory for Nanophotonics, Rice University, Houston, Texas 77005, USA

<sup>3</sup>Department of Electrical and Computer Engineering, Laboratory for Nanophotonics, Rice University, Houston, Texas 77005, USA

<sup>4</sup>Division of Solid State Physics/The Nanometer Consortium, Lund University, P.O. Box 118, S-22100 Lund, Sweden

(Received 9 September 2010; published 3 December 2010)

We investigate how the properties of a nearby substrate modify the excitation and propagation of plasmons in subwavelength silver wires. With decreasing nanowire-substrate separation, the in-coupling efficiency shows strongly oscillatory behavior due to coherent interference. The plasmon damping increases with decreasing separation due to an increased coupling of the nanowire plasmons to the photonic modes of the substrate.

DOI: [10.1103/PhysRevB.82.241402](https://doi.org/10.1103/PhysRevB.82.241402)

PACS number(s): 73.20.Mf, 42.82.Et, 78.67.Uh

Surface-plasmons polaritons (SPPs) can propagate in sub-wavelength structures of widths that can be scaled down to a few tens of nanometer.<sup>1–5</sup> Various subwavelength plasmonic devices have already been developed, such as nanolasers,<sup>6</sup> modulators,<sup>7</sup> splitters,<sup>8–10</sup> detectors,<sup>11</sup> and polarization rotators.<sup>12–14</sup> Plasmonic waveguiding is a possible solution to the interconnect problem between components in future integrated circuits, offering vastly improved bandwidth relative to traditional electrical interconnects.<sup>15</sup> Much recent work on plasmonic waveguides has focused on chemically synthesized metallic nanowires, which support plasmon propagation with minimum loss.<sup>1,8,11,12,16–22</sup> For efficient plasmonic waveguiding, it is important to minimize the loss inherent in the in- and out-coupling efficiencies between photons and plasmons and during plasmon propagation in the waveguide.<sup>9,23–27</sup> Several investigations of loss mechanisms have been performed,<sup>24,25</sup> but to our knowledge, no previous investigation has addressed the possibilities of loss induced by energy transfer into the substrate. This is clearly an important issue since plasmonic waveguides and devices are almost universally fabricated or deposited on substrates of various dielectric or semiconducting media.

Here we investigate plasmon propagation in Ag nanowires positioned at different separations from dielectric substrates of various compositions. We find that both the in-coupling efficiency of light into nanowire SPPs and the damping of the propagating plasmon depend sensitively on the proximity of the nanowire to the substrate and on the dielectric permittivity of the substrate.<sup>28–30</sup> While the damping of the propagating plasmon decreases monotonically with increasing nanowire-substrate separation, the in-coupling efficiency exhibits a surprisingly nonmonotonic behavior, peaking at specific nanowire-substrate separations related to the interference between the incident light and reflected light from the substrate. The damping of the propagating plasmon influenced by the substrate can be understood as resulting from interactions between the nanowire and the substrate.

Chemically synthesized Ag nanowires<sup>31</sup> were deposited on Si substrates with SiO<sub>2</sub> surface spacer layers of varying thicknesses. The nanowire was then embedded in immersion oil with a refractive index matched to the silica layer. Thus the silica layer is negligible optically and serves only as a

passive spacer layer. SPPs are launched at one end of the nanowire by a diffraction-limited 633 nm laser spot focused by an oil immersion objective (Olympus UPlanApo, 100×, NA=1.35). The polarization of the incident laser is rotated to be parallel to the nanowire axis by a half-wave plate to ensure maximum emission intensity. The emission intensity from the other end of the nanowire is recorded by a TE cooled 1392 × 1040 charge-coupled-device detector. The diameter of each nanowire is measured by scanning electron microscopy.

The emission intensities from nanowires of diameter in the range  $D=90–100$  nm, for three separations, are shown in Fig. 1(a). It is clearly seen that nanowires of similar lengths on a thick SiO<sub>2</sub> spacer layer ( $d=110$  nm) usually emit light more strongly than nanowires on a thin layer ( $d=67$  nm). For silica layers of thickness less than 41 nm, there is almost no observable emission from the nanowire end. It should be noted that the measured data are still significantly scattered around the fitting line even when the distribution of nanowire diameters is narrowed to  $D=95–100$  nm. This scatter is mainly caused by the strong sensitivity of the SPP Fabry-Pérot resonances to slight variations in nanowire diameters and lengths, as reported previously.<sup>20</sup> Various shapes of nanowire terminations can also cause discrepancies in the emission intensity from nanowires with similar length and diameter.<sup>20</sup>

To understand the strong dependence of nanowire emission on spacer layer thickness, we parametrize the emission intensity  $I_e$  as

$$I_e = I_0 C(d) e^{-L/r(D,d)}, \quad (1)$$

where  $L$  is the length of the nanowire,  $I_0$  is the incident intensity,  $C(d)$  is the in-coupling coefficient, and  $r(D,d)$  is the  $1/e$  damping length of the nanowire SPPs.

In Fig. 1(b), the average emission intensity from nanowires of similar length  $L=4–4.5$  μm and diameter  $D=90–100$  nm on layered substrates as a function of silica layer thickness  $d$ , normalized it to maximum emission in each case, is shown. It is interesting that the average emission intensity exhibits a strongly nonmonotonic behavior, with maxima occurring at  $d \sim 110$  and 300 nm, decreasing very strongly as  $d$  is reduced to zero thickness. Figures 1(c)

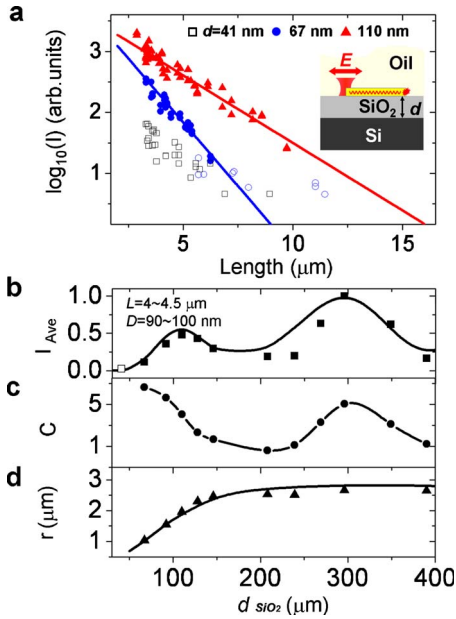


FIG. 1. (Color online) (a) Emission intensities from nanowires on layered substrates as a function of nanowire length  $L$ . The diameters of all nanowires were selected to be in the range  $D = 90\text{--}100$  nm. Inset: a schematic of the experimental measurement. Incident light of wavelength 633 nm, polarized parallel to the nanowire, is directed onto one end of the nanowire. Light emitted from the other end is measured for various nanowire lengths  $L$  and silica layer thicknesses  $d = 41, 67,$  and  $110$  nm. When there is no observable light emission, the scattered light at the end of the nanowire is recorded and represented by hollow dots. (b) Average emission intensity for nanowires (black squares) of length  $L = 4\text{--}4.5$   $\mu\text{m}$  and diameter  $D = 90\text{--}100$  nm as a function of the silica layer thickness  $d$ . The curve is the theoretical simulation (FDTD) of this geometry. (c) In-coupling coefficient  $C$  as a function of silica thickness  $d$ . The unit for  $I_{\text{Ave}}$  and  $C$  in (b) and (c) is arbitrary. (d)  $1/e$  damping length of SPPs as a function of  $d$ . The curve is the calculated  $r$  divided by 1.4, discussed in the text. The refractive index of silicon is 3.882. The refractive of the oil is index matched to silica  $n_s = 1.518$ .

and 1(d) show the in-coupling coefficient  $C(d)$  and  $1/e$  damping length  $r(D, d)$  of SPPs in nanowires on layered substrates obtained by fitting the experimental data to Eq. (1). The in-coupling coefficient  $C$  is large for  $d = 40$  nm, then decreases for increasing  $d$  until  $d \sim 200$  nm, then increases and peaks for  $d \sim 300$  nm, and then decreases. The damping length  $r(D, d)$ , on the other hand, increases monotonically with increasing silica thickness and saturates beyond  $d > 200$  nm. The combined effect of increased in-coupling efficiency but decreased propagation length due to increased substrate coupling for small nanowire-substrate separations leads to an overall maximum in light emission at  $d \sim 110$  nm [Fig. 1(b)].

To understand the effect of the substrate on in-coupling efficiency and propagation length, electromagnetic simulations using finite-difference time-domain (FDTD)-based commercial software (LUMERICAL) were performed. Figure 2(a) shows the field distribution around a nanowire for  $d = 100$  nm. It is clear that propagating SPPs are launched along the nanowire. Due to the superposition of the incident

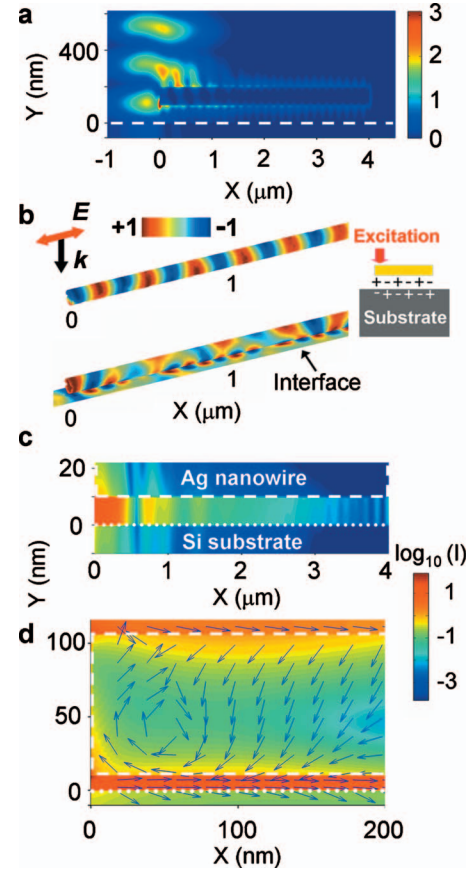


FIG. 2. (Color) (a) The field distribution ( $|E|^2$ ) around the nanowire of diameter 96 nm, length 4  $\mu\text{m}$ , and  $d = 100$  nm excited by a 633 nm laser with parallel polarization relative to the wire axis at the left end. (b) The plasmon-induced surface charge amplitude on the nanowire without and with adjacent Si surface ( $d = 10$  nm). The charge is obtained by the divergence of the electric field. The unit of charge is arbitrary from +1 to  $-1$  corresponding to color from red to blue. (c) The intensity of the electric field confined in the wire-substrate gap in (b) on a logarithmic scale. (d) The Poynting vector/electromagnetic energy flow around the first 200 nm of the wire and the wire-substrate gap. Arrows denotes the direction of the flow; the color represents the local electric intensity.

and substrate-reflected light, standing waves are formed in the vertical direction ( $y$  direction). The first two antinodes of standing waves are located at approximately 100 and 300 nm in the  $y$  direction. As the thickness of the spacer layer is increased, the excitation end of the nanowire moves across these two antinodes, enabling more efficient in-coupling and thus enhanced light emission [Figs. 1(b) and 1(c)]. The calculated emission intensity from a nanowire of length  $L = 4$   $\mu\text{m}$  and diameter  $D = 96$  nm, shown in Fig. 1(b), agrees very well with the experimental data.

For  $d < 200$  nm, when the nanowire is close to the Si substrate, the in-coupling coefficient  $C$  shown in Fig. 1(c) increases dramatically. Although this means that more light can be coupled to SPPs in the nanowires for larger  $C$ , the proximity of the nanowire to the substrate results in significantly more damping, as evidenced by the reduced damping length  $r$  shown in Fig. 1(d).

To understand the strong decrease in propagation length

with decreasing spacer layer thickness, we calculate the plasmon-induced surface charge on the surface of a silver nanowire and the induced surface charges at the silicon interface for a thin  $d=10$  nm silica spacer layer [Fig. 2(b)]. Here the large induced surface charges at the silicon interface represent a strong coupling to the nanowire plasmon, which results in the wavelength of the propagating plasmons being reduced to  $\sim 200$  nm, in comparison with the case of a free wire without substrate ( $\lambda_{\text{plasmons}} \sim 320$  nm). The charge distribution in the substrate can confine the plasmon modes in the gap between the nanowire and the silicon surface,<sup>32,33</sup> as indicated in Fig. 2(c). Figure 2(d) shows the Poynting vector/electromagnetic energy flow in the gap and wire. It is clear that the photons can propagate in the wire-substrate gap, i.e., that, the gap mode is excited. When  $d$  is decreased, the resonance of the gap mode is redshifted and results in larger propagation damping. By calculating the energy flow along the nanowire for different separations, the corresponding SPP damping lengths are extracted and plotted with the black curve in Fig. 1(c). The calculated values are about 40% larger than the experimental values. This discrepancy may be caused by uncertainties in the silver dielectric function used in calculation,<sup>34</sup> or may also be due to the presence of defects in the chemically synthesized nanowires. For  $d < 40$  nm, the damping of the nanowire plasmons becomes so large that the resulting emission intensity from the nanowire end becomes very weak. This may be the reason why no light emission was detected at the distal end of the nanowire and only the light scattered by the wire end could be detected, as shown by the hollow squares in Fig. 1(a). Further analysis shows that the substrate-induced damping length approximately follows the relation,  $r = r_0 e^{-\eta^3/d^3}$  in the range of  $40 < d < 400$  nm, where  $r_0$  is the SPPs damping length without substrate,  $\eta = d_0(\epsilon - \epsilon_s)/(\epsilon + \epsilon_s)$ , where  $\epsilon$  and  $\epsilon_s$  are the real part of the permittivities of the substrate and of the dielectric surroundings, respectively. The best fit to the experimental data is obtained for  $d_0 = 98$  nm.

Since silicon with its indirect band gap around 1.1 eV has a weak absorption at 633 nm (1.96 eV), one might suspect that the substrate-induced damping may originate from direct absorption in the silicon substrate. To test this hypothesis, we measure the emission intensity from nanowires on a GaP substrate (band gap 2.26 eV) which has a similar refractive index  $n=3.31$  to silicon but no absorption at 633 nm. As shown by the hollow triangles in Fig. 3(a), there is no observable emission from the nanowire end on the GaP substrate, similar to the result for nanowires near the silicon substrate. This observation shows that substrate-induced damping is due to primarily to conversion of plasmons into photonic modes of the substrate, not by weak electron-hole excitations in the substrate. This result is also confirmed by the calculated damping length of SPPs as a function of substrate refractive index, shown in Fig. 3(b). The damping length decreases with the increase in the refractive index of the substrate due to increasing nanowire-substrate coupling. For a substrate with  $n > 3$ , the coupling to the substrate is so strong to become saturated and not dependent on  $n$ , the damping length is reduced to a constant  $r \sim 0.6$   $\mu\text{m}$ . That is the main cause for the kink observed when  $n > 3$ .

Conversely, the effect of strongly absorptive substrates on

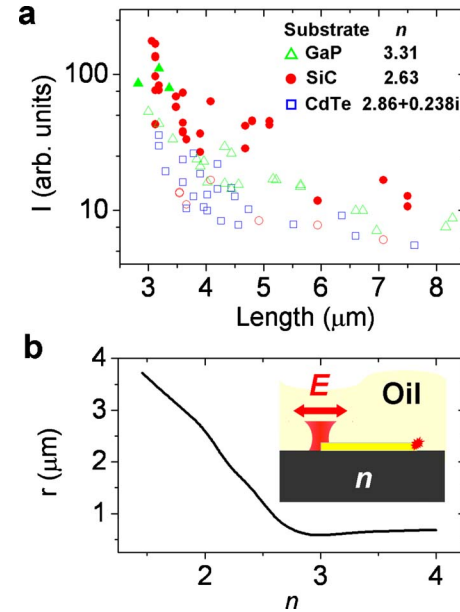


FIG. 3. (Color online) (a) The measured emission intensity from nanowires of diameters  $D=90-100$  nm on different substrates as a function of the nanowire length. The excitation with the wavelength 633 nm at one of the nanowire is always polarized parallel to the nanowire. Triangular, circular, and squared dots represent the cases of nanowires on substrates of GaP, SiC, and CdTe, respectively. For cases with no observable light emission at the end of the nanowire, scattered light at the position of the nanowire end was recorded and represented by hollow dots. (b) The calculated damping length as a function of the refractive index of the substrate.

the damping length  $r$  can be large, which can be seen by comparing nanowire plasmon propagation for nanowires placed in direct contact ( $d=0$ ) on silicon carbide (SiC band gap 3.03 eV) and cadmium telluride (CdTe band gap 1.5 eV) substrates. The real part of the refractive index of these two materials are similar but CdTe absorbs strongly at 633 nm (for SiC  $n=2.63$  and CdTe  $n=2.86+0.238i$ ). Figure 3(a) shows that while SPPs can propagate efficiently on nanowires on the SiC substrate (circles), no observable light emission occurs for nanowires on the CdTe substrate (hollow squares). The calculated damping length of plasmons on nanowires on a SiC substrate is  $\sim 1.4$  times larger than for the CdTe substrate. The absorption caused by band-gap excitations of the CdTe substrate thus induces an additional decay channel for SPPs.

In conclusion, we have measured the emission intensity of SPPs launched in individual silver nanowires at different separations from different substrates. We find that both the in-coupling efficiency and the damping length of the nanowire plasmons are influenced by the presence of a nearby substrate. The in-coupling efficiency can exhibit strong peaks for certain wire-substrate separations due to the interference between incident and reflected light. In contrast, coupling to the substrate makes the decay length of nanowire plasmons decrease monotonically with decreasing wire-substrate separation. This coupling depends on wire-substrate separation and the dielectric permittivity of the substrate. For strongly absorbing substrates, the substrate-induced damping can be

very large. The understanding of the propagating properties of surface plasmons on substrates is important for the development of nanoscale photonic devices.

We thank Xiaolong Chen for providing the SiC substrate and Yingzhou Huang and Fengzi Cong for the help with sample preparation. This work was supported by NSFC under Grants No. 10625418, No. 10874233, and No. 10904171,

MOST under Grants No. 2006DFB02020 and No. 2009CB930700, “Bairen Project” of CAS, the National Science Foundation under Grant No. CNS-0421109, the Robert A Welch Foundation under Grants No. C-1220 and No. C-1222, and the Center for Advanced Solar Photophysics, an Energy Frontier Research Center funded by the U.S. Department of Energy, Office of Science, Office of Basic Energy Sciences.

\*Corresponding author.

†nordland@rice.edu

‡hxxu@aphy.iphy.ac.cn

- <sup>1</sup>H. Ditlbacher, A. Hohenau, D. Wagner, U. Kreibig, M. Rogers, F. Hofer, F. R. Aussenegg, and J. R. Krenn, *Phys. Rev. Lett.* **95**, 257403 (2005).
- <sup>2</sup>E. Ozbay, *Science* **311**, 189 (2006).
- <sup>3</sup>G. W. Bryant, F. J. García de Abajo, and J. Aizpurua, *Nano Lett.* **8**, 631 (2008).
- <sup>4</sup>R. F. Oulton, V. J. Sorger, D. A. Genov, D. F. P. Pile, and X. Zhang, *Nat. Photonics* **2**, 496 (2008).
- <sup>5</sup>J. Dorfmueller, R. Vogelgesang, R. T. Weitz, C. Rockstuhl, C. Etrich, T. Pertsch, F. Lederer, and K. Kern, *Nano Lett.* **9**, 2372 (2009).
- <sup>6</sup>M. A. Noginov, G. Zhu, A. M. Belgrave, R. Bakker, V. M. Shalaev, E. E. Narimanov, S. Stout, E. Herz, T. Suteewong, and U. Wiesner, *Nature (London)* **460**, 1110 (2009).
- <sup>7</sup>W. S. Cai, J. S. White, and M. L. Brongersma, *Nano Lett.* **9**, 4403 (2009).
- <sup>8</sup>R. X. Yan, P. Pausauskie, J. X. Huang, and P. D. Yang, *Proc. Natl. Acad. Sci. U.S.A.* **106**, 21045 (2009).
- <sup>9</sup>X. Guo, M. Qiu, J. M. Bao, B. J. Wiley, Q. Yang, X. N. Zhang, Y. G. Ma, H. K. Yu, and L. M. Tong, *Nano Lett.* **9**, 4515 (2009).
- <sup>10</sup>Y. R. Fang, Z. P. Li, Y. Z. Huang, S. P. Zhang, P. Nordlander, N. J. Halas, and H. X. Xu, *Nano Lett.* **10**, 1950 (2010).
- <sup>11</sup>Y. R. Fang, H. Wei, F. Hao, P. Nordlander, and H. X. Xu, *Nano Lett.* **9**, 2049 (2009).
- <sup>12</sup>Z. P. Li, K. Bao, Y. R. Fang, Y. Z. Huang, P. Nordlander, and H. X. Xu, *Nano Lett.* **10**, 1831 (2010).
- <sup>13</sup>T. Shegai, Z. P. Li, T. Dadoosh, Z. Zhang, H. X. Xu, and G. Haran, *Proc. Natl. Acad. Sci. U.S.A.* **105**, 16448 (2008).
- <sup>14</sup>Z. P. Li, T. Shegai, G. Haran, and H. X. Xu, *ACS Nano* **3**, 637 (2009).
- <sup>15</sup>X. F. Duan, Y. Huang, Y. Cui, J. F. Wang, and C. M. Lieber, *Nature (London)* **409**, 66 (2001).
- <sup>16</sup>A. W. Sanders, D. A. Routenberg, B. J. Wiley, Y. N. Xia, E. R. Dufresne, and M. A. Reed, *Nano Lett.* **6**, 1822 (2006).
- <sup>17</sup>A. V. Akimov, A. Mukherjee, C. L. Yu, D. E. Chang, A. S. Zibrov, P. R. Hemmer, H. Park, and M. D. Lukin, *Nature (London)* **450**, 402 (2007).
- <sup>18</sup>M. W. Knight, N. K. Grady, R. Bardhan, F. Hao, P. Nordlander, and N. J. Halas, *Nano Lett.* **7**, 2346 (2007).
- <sup>19</sup>A. Manjavacas and F. J. García de Abajo, *Nano Lett.* **9**, 1285 (2009).
- <sup>20</sup>Z. P. Li, F. Hao, Y. Z. Huang, Y. R. Fang, P. Nordlander, and H. X. Xu, *Nano Lett.* **9**, 4383 (2009).
- <sup>21</sup>H. Wei, D. Ratchford, X. Q. Li, H. X. Xu, and C. K. Shih, *Nano Lett.* **9**, 4168 (2009).
- <sup>22</sup>T. Shegai, Y. Huang, H. Xu, and M. Käll, *Appl. Phys. Lett.* **96**, 103114 (2010).
- <sup>23</sup>W. L. Barnes, A. Dereux, and T. W. Ebbesen, *Nature (London)* **424**, 824 (2003).
- <sup>24</sup>J. A. Dionne, L. A. Sweatlock, H. A. Atwater, and A. Polman, *Phys. Rev. B* **72**, 075405 (2005).
- <sup>25</sup>R. Zia, J. A. Schuller, and M. L. Brongersma, *Phys. Rev. B* **74**, 165415 (2006).
- <sup>26</sup>R. Zia, J. A. Schuller, A. Chandran, and M. L. Brongersma, *Mater. Today* **9**, 20 (2006).
- <sup>27</sup>D. E. Chang, A. S. Sorensen, P. R. Hemmer, and M. D. Lukin, *Phys. Rev. Lett.* **97**, 053002 (2006).
- <sup>28</sup>Z. L. Wang and J. M. Cowley, *Ultramicroscopy* **23**, 97 (1987).
- <sup>29</sup>Y. H. Yu, Y. Jiang, Z. Tang, Q. L. Guo, J. F. Jia, Q. K. Xue, K. H. Wu, and E. G. Wang, *Phys. Rev. B* **72**, 205405 (2005).
- <sup>30</sup>A. Politano, R. G. Agostino, E. Colavita, V. Formoso, and G. Chiarello, *Phys. Status Solidi (RRL)* **2**, 86 (2008).
- <sup>31</sup>Y. G. Sun, B. Mayers, T. Herricks, and Y. N. Xia, *Nano Lett.* **3**, 955 (2003).
- <sup>32</sup>H. X. Xu and M. Kall, *Sens. Actuators B* **87**, 244 (2002).
- <sup>33</sup>M. W. Knight, Y. P. Wu, J. B. Lassiter, P. Nordlander, and N. J. Halas, *Nano Lett.* **9**, 2188 (2009).
- <sup>34</sup>P. B. Johnson and R. W. Christy, *Phys. Rev. B* **6**, 4370 (1972).